Hidden Histidine Radical Rearrangements upon Electron Transfer to Gas-Phase Peptide Ions. Experimental Evidence and Theoretical Analysis

ARTICLE *in* JOURNAL OF THE AMERICAN CHEMICAL SOCIETY · NOVEMBER 2008

Impact Factor: 12.11 · DOI: 10.1021/ja8036367 · Source: PubMed

7 AUTHORS, INCLUDING:

Frantisek Turecek
University of Washington Seattle
237 PUBLICATIONS **9,698** CITATIONS
SEE PROFILE

Subhasis Panja
National Physical Laboratory - India
50 PUBLICATIONS **821** CITATIONS
SEE PROFILE

Steen Brøndsted Nielsen
Aarhus University
197 PUBLICATIONS **3,075** CITATIONS
SEE PROFILE

Preben Hvelplund
Aarhus University
58 PUBLICATIONS **1,001** CITATIONS
SEE PROFILE

J|A|C|S
ARTICLES

Published on Web 10/11/2008

Hidden Histidine Radical Rearrangements upon Electron Transfer to Gas-Phase Peptide Ions. Experimental Evidence and Theoretical Analysis

František Tureček,*,† Jace W. Jones,† Tyrell Towle,† Subhasis Panja,‡ Steen Brøndsted Nielsen,‡ Preben Hvelplund,‡ and Bela Paizs§

Department of Chemistry, Bagley Hall, Box 351700, University of Washington, Seattle, Washington 98195-1700, Department of Physics and Astronomy, University of Aarhus, Aarhus, Denmark, and Department of Molecular Biophysics, German Cancer Research Center, Im Neuenheimer Feld 580, D-69120 Heidelberg, Germany

Received May 15, 2008; E-mail: turecek@chem.washington.edu

Abstract: Protonated peptides containing histidine or arginine residues and a free carboxyl group (His-Ala-Ile, His-Ala-Leu, Ala-His-Leu, Ala-Ala-His-Ala-Leu, His-Ala-Ala-Ala-Leu, and Arg-Ala-Ile) form stable anions upon collisional double electron transfer from Cs atoms at 50 keV kinetic energies. This unusual behavior is explained by hidden rearrangements occurring in peptide radical intermediates formed by transfer of the first electron. The rearrangements occur on a ~120 ns time scale determined by the radical flight time. Analysis of the conformational space for (His-Ala-Ile + H)$^+$ precursor cations identified two major conformer groups, **1a**$^+$−**1m**$^+$ and **5a**$^+$−**5h**$^+$, that differed in their H-bonding patterns and were calculated to collectively account for 39% and 60%, respectively, of the gas-phase ions. One-electron reduction in **1a**$^+$ and **5a**$^+$ triggers exothermic hydrogen atom migration from the terminal COOH group onto the His imidazole ring, forming imidazoline radical intermediates. The intermediate from **5a** is characterized by its charge and spin distribution as a novel cation radical−COO$^-$ salt bridge. The intermediate from **1a** undergoes spontaneous isomerization by imidazoline N−H migration, re-forming the COOH group and accomplishing exothermic isomerization of the initial (3*H*)-imidazole radical to a (2*H*)-imidazole radical. An analogous unimolecular isomerization in simple imidazole and histidine radicals requires activation energies of 150 kJ mol^{-1}, and its occurrence in **1a** and **5a** is due to the promoting effect of the proximate COOH group. The rearrangement is substantially reduced in Ala-Leu-His due to an unfavorable spatial orientation of the imidazole and COOH groups and precluded in the absence of a free carboxyl group in His-Ala-Leu amide. In contrast to His-Ala-Ile and Arg-Ala-Ile, protonated Lys-Ala-Ile does not produce stable anions upon double electron transfer. The radical trapping properties of histidine residues are discussed.

Introduction

Electron-based methods of ion dissociation[1] have been of much recent interest because of their potential for peptide sequencing,[2] determination of post-translational modifications,[3] detection of protein aging,[4] and applications to other biological processes.[2b] When applied to biomolecules, electron-based methods use multiply charged ions produced by electrospray ionization that are subjected to recombination with low-energy electrons, electron transfer in ion−ion reactions with selected molecular anions, or femtosecond electron transfer from neutral targets, such as alkali-metal atoms. These processes form charge-reduced, open-electron shell intermediates which undergo dissociations called, respectively, electron capture dissociation (ECD),[2] electron transfer dissociation (ETD),[5] and electron capture induced dissociation (ECID),[6] resulting in losses of atoms and small molecules. Perhaps most importantly, charge-reduced peptide ions also undergo backbone dissociations that mainly affect the bonds between the amide nitrogen and C-terminal α-carbon atoms, the N−C$_\alpha$ bond cleavage.[2] These bond dissociations produce fragments of the **c** and **z** type

† University of Washington.
‡ University of Aarhus.
§ German Cancer Research Center.

(1) For a recent review see: (a) Tureček, F. *Top. Curr. Chem.* **2003**, *225*, 77–129.

(2) (a) Zubarev, R. A.; Kelleher, N. L.; McLafferty, F. W. *J. Am. Chem. Soc.* **1998**, *120*, 3265–3266. (b) Zubarev, R. A.; Horn, D. M.; Fridriksson, E. K.; Kelleher, N. L.; Kruger, N. A.; Lewis, M. A.; Carpenter, B. K.; McLafferty, F. W. *Anal. Chem.* **2000**, *72*, 563–573. (c) Cooper, H. J.; Hakansson, K.; Marshall, A. G. *Mass Spectrom. Rev.* **2005**, *24*, 201–222.

(3) (a) Stensballe, A.; Jensen, O. N.; Olsen, J. V.; Haselmann, K. F.; Zubarev, R. A. *Rapid Commun. Mass Spectrom.* **2000**, *14*, 1793–1800. (b) Mirgorodskaya, E.; Roepstorff, P.; Zubarev, R. A. *Anal. Chem.* **1999**, *71*, 4431–4436. (c) Sze, S. K.; Ge, Y.; Oh, H. B.; McLafferty, F. W. *Proc. Natl. Acad. Sci. U.S.A.* **2002**, *99*, 1774–1779. (d) Kelleher, N. L.; Zubarev, R. A.; Bush, K.; Furie, B.; Furie, B. C.; McLafferty, F. W.; Walsh, C. T. *Anal. Chem.* **1999**, *71*, 4250–4253. (e) Ge, Y.; Lawhorn, B. G.; ElNaggar, M.; Strauss, E.; Park, J.-H.; Begley, T. P.; McLafferty, F. W. *J. Am. Chem. Soc.* **2002**, *124*, 672–678.

(4) (a) Cournoyer, J. J.; Pittman, J. L.; Ivleva, V. B.; Fallows, E.; Waskell, L.; Costello, C. E.; O'Connor, P. B. *Protein Sci.* **2005**, *14*, 452–463. (b) Cournoyer, J. J.; Lin, C.; O'Connor, P. B. *Anal. Chem.* **2006**, *78*, 1264–1271. (c) O'Connor, P. B.; Cournoyer, J. J.; Pitteri, S. J.; Chrisman, P. A.; McLuckey, S. A. *J. Am. Soc. Mass Spectrom.* **2006**, *17*, 15–19. (d) Cournoyer, J. J.; Lin, C.; Bowman, M. J.; O'Connor, P. B. *J. Am. Soc. Mass Spectrom.* **2007**, *18*, 48–56.

 10.1021/ja8036367 CCC: $40.75

Scheme 1

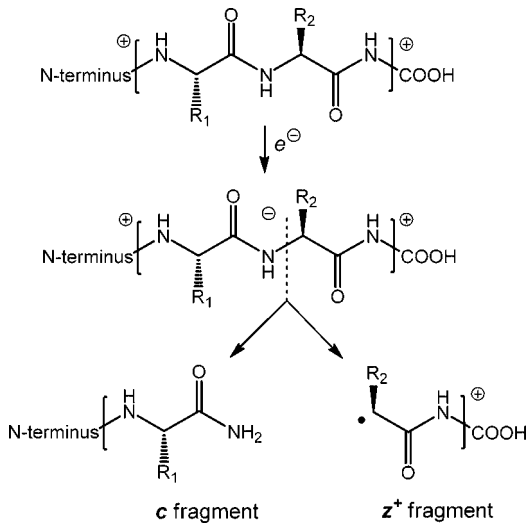

(Scheme 1), which are different from fragments formed by collisional activation or infrared photoexcitation of closed-shell cations. Typically, N−C_α bonds at various positions are cleaved in charge-reduced peptide cation radicals upon ECD or ETD, consistent with the extremely low transition-state energies for the bond cleavage in peptide radicals[7] and exothermic dissociations that form ion−molecule complexes between the incipient **c** and **z** fragments.[8]

The effects on dissociations of peptide amino acid type and sequence have been studied for ECD[9] and ETD,[10] and interesting results have been reported. In particular, electron transfer to histidine- and arginine-containing peptides has been found to produce substantial fractions of nondissociating charge-reduced ions of unknown structure. Arginine is often found as a C-terminal residue in peptides produced by protein trypsinolysis, and analysis of such peptides is important for bottom-up proteomics. We have reported that radicals formed by electron transfer to protonated arginine,[11] arginine amide,[12] and arginine-containing dipeptides[13] underwent hydrogen transfer from the C_α position onto the guanidinium carbon atom, which occurred in competition with side-chain dissociations. This so-called arginine anomaly[12] produced stable radical intermediates that were detected if they carried a charge or following ionization. The structures of rearranged arginine radicals have been established by a combination of ab initio calculations and charge-inversion ($^+CR^-$) experiments.[14] In the latter, the intermediate radicals were formed by femtosecond collisional electron transfer to singly protonated peptides, and the radicals were probed by electron transfer in a second collision to form negative ions. Negative ions owe their stability to positive electron affinities of the pertinent radicals. Thus, electron affinities provide a straightforward determinant for the selection of radical structures that may be observable on the time scale of ECID experiments.[15] In addition, $^+CR^-$ experiments allow one to investigate ion structures for singly protonated peptides which are not amenable to ECD or ETD and thus gain insight about their redox chemistry in the absence of residual charge.

We now apply this selective method to probe structures of radical intermediates formed by electron transfer to singly protonated tripeptides containing His, Arg, and Lys residues. Histidine is a relatively rare amino acid which appears in 2.2−2.3% of known protein sequences,[16] but is an essential component of about 50 redox and hydrolytic enzymes such as dehydrogenases, kinases, phosphatases, sulfatases, ribonucleases, and amino- and carboxypeptidases.[17] Tripeptide models His-Ala-Ile (HAI), His-Ala-Leu (HAL), Arg-Ala-Ile (RAI), and Lys-Ala-Ile (KAI) have the same sequence of hydrophobic amino acids, but differ in the basic amino acid at the N-terminus. We also investigate the effect of the His residue position in the peptide chain in AHL, ALH, AAHAL, and HAAAL and the effect caused by absence of a free carboxyl group in HAL-NH_2.

The His, Arg, and Lys amino acid residues steer protonation to the basic groups in their respective side chains to provide unequivocal chemical structures for the precursor ions. Full conformational analysis has been carried out for the representative $(HAI + H)^+$ system to establish precursor ion secondary structures. We investigate the formation of stable radicals upon electron transfer in competition with backbone dissociations using selective detection of stable anions from neutral intermediates. We show that histidine and, to a lesser extent, arginine residues undergo hidden rearrangements by hydrogen migrations that can explain the experimental observations and provide a new paradigm for thinking about electron-based peptide dissociations.

Experimental Part

Materials and Methods. The tripeptides HAI, HAL, KAI, KAL, RAI, and RAL were synthesized as free acids using an automatic peptide synthesizer (ResPep MicroScale, Intavis AG, Köln, Ger-

(5) (a) Syka, J. E. P.; Coon, J. J.; Schroeder, M. J.; Shabanowitz, J.; Hunt, D. F. *Proc Natl. Acad. Sci. U.S.A.* **2004**, *101*, 9528–9533. (b) Coon, J. J.; Syka, J. E. P.; Schwartz, J. C.; Shabanowitz, J.; Hunt, D. F. *Int. J. Mass Spectrom.* **2004**, *236*, 33–42. (c) Coon, J. J.; Ueberheide, B.; Syka, J. E. P.; Dryhurst, D. D.; Ausio, J.; Shabanowitz, J.; Hunt, D. F. *Proc. Natl. Acad. Sci. U.S.A.* **2005**, *102*, 9463–9468. (d) Pitteri, S. J.; Chrisman, P. A.; Hogan, J. M.; McLuckey, S. A. *Anal. Chem.* **2005**, *77*, 1831–1839. (e) Gunawardena, H. P.; He, M.; Chrisman, P. A.; Pitteri, S. J.; Hogan, J. M.; Hodges, B. D. M.; McLuckey, S. A. *J. Am. Chem. Soc.* **2005**, *127*, 12627–12639. (f) Srikanth, R.; Wilson, J.; Bridgewater, J. D.; Numbers, J. R.; Lim, J.; Olbris, M. R.; Kettani, A.; Vachet, R. W. *J. Am. Soc. Mass Spectrom.* **2007**, *18*, 1499–1506.
(6) (a) Boltalina, O. V.; Hvelplund, P.; Jørgensen, T. J. D.; Larsen, M. C.; Larsson, M. O.; Sharoitchenko, D. A.; Sørensen, M. *Phys. Rev. A* **2000**, *62*, 023202. (b) Larsson, M. O.; Hvelplund, P.; Larsen, M. C.; Shen, H.; Cederquist, H.; Schmidt, H. T. *Int. J. Mass Spectrom.* **1998**, *177*, 51–62.
(7) Tureček, F.; Syrstad, E. A. *J. Am. Chem. Soc.* **2003**, *125*, 3353–3369.
(8) (a) Tureček, F. *J. Am. Chem. Soc.* **2003**, *125*, 5954–5963. (b) Tureček, F.; Syrstad, E. A.; Seymour, J. L.; Chen, X.; Yao, C. *J. Mass Spectrom.* **2003**, *38*, 1093–1104.
(9) (a) Iavarone, A. T.; Paech, K.; Williams, E. R. *Anal. Chem.* **2004**, *76*, 2231–2238. (b) Savitski, M. M.; Kjeldsen, F.; Nielsen, M. L.; Zubarev, R. A. *Angew. Chem., Int. Ed.* **2006**, *45*, 5301–5303.
(10) Xia, Y.; Gunawardena, H. P.; Erickson, D. E.; McLuckey, S. A. *J. Am. Chem. Soc.* **2007**, *129*, 12232–12243.
(11) Hayakawa, S.; Matsubara, H.; Panja, S.; Hvelplund, P.; Nielsen, S. B.; Chen, X.; Tureček, F. *J. Am. Chem. Soc.* **2008**, *130*, 7645–7654.
(12) Chen, X.; Turecek, F. *J. Am. Chem. Soc.* **2006**, *128*, 12520–12530.
(13) Panja, S.; Nielsen, S. B.; Hvelplund, P.; Tureček, F. *J. Am. Soc. Mass Spectrom.*, in press.
(14) (a) Schroder, D. Charge Reversal. In *The Encyclopedia of Mass Spectrometry*; Armentrout, P. B., Ed.; Elsevier: Amsterdam, 2003; Vol. 1, Chapter 8, pp 521−528. (b) Hayakawa, S. *J. Mass Spectrom.* **2004**, *39*, 111–135.
(15) (a) Hayakawa, S.; Hashimoto, M.; Matsubara, H.; Tureček, F. *J. Am. Chem. Soc.* **2007**, *129*, 7936–7949. (b) Hvelplund, P.; Liu, B.; Nielsen, S.; Brøndsted Tomita, S. *Int. J. Mass Spectrom.* **2003**, *225*, 83–87. (c) Hvelplund, P.; Liu, B.; Nielsen, S.; Brøndsted Panja, S.; Poully, J.-C.; Støchkel, K. *Int. J. Mass Spectrom.* **2007**, *263*, 66–70.
(16) Trinquier, G.; Sanejouand, Y.-H. *Protein Eng.* **1998**, *11*, 153–169.
(17) Schneider, F. *Angew. Chem., Int. Ed. Engl.* **1978**, *17*, 583–592.

many) according to the F-moc synthesis strategy. Peptides AHL, ALH, HAL-amide, AAHAL, and HAAAL (>95% purity) were purchased from GenScript (Piscataway, NJ). The peptides were characterized by electrospray mass spectrometry (ESI-MS) in combination with collision-induced dissociation of the respective $(M + H)^+$ ions (MS/MS) to verify the amino acid sequence. ESI-MS and MS/MS were measured on an Esquire LC ion trap mass spectrometer (Bruker, Daltonics, Billerica, MA) equipped with an electrospray ion source. The sample solution in water−methanol was directly infused into the ion source at a flow rate of 1.5 μL/min. The parameters for the ion source and mass spectrometer were as follows: capillary voltage, −4000 V; end plate, 500 V; capillary offset, 100 V; skimmer 1 set at 30 V; skimmer 2 set at 4 V; octopole, 3 V, trap drive, 55−80 V; ion charge control on with target 25 000 ions; nebulizing gas (N_2), 9.0 psi; drying gas (N_2), 3 L/min; drying temperature, 250 °C. MS/MS spectra were collected with an isolation width of 4 u and the fragmentation amplitude set to 1 V. The mass accuracy of the data was ±0.3 u. Charge inversion mass spectra were measured on a large-scale sector instrument described previously.[6] Briefly, the instrument consists of an electrospray ionization source and a three-stage pumping system which are mounted on a high-voltage platform floated at 50 kV.

Ions produced in the source are accelerated to $50z$ keV (z = ion charge) and separated by a double-focusing magnetic sector of 2 m radius and 72° deflection angle. The magnetic sector achieves a 1364 $\Delta M/M$ dispersion in the focal plane at the mass-resolving slit. Mass-selected ions enter a special differentially pumped collision cell which contains a resistively heated reservoir of Cs. The partial pressure of Cs vapor is controlled by adjusting the reservoir temperature. Products of ion−Cs collisions pass a variable-width energy-resolving slit and travel to a 180° electrostatic analyzer which is located 80 cm after the collision cell. Energy-resolved ions are detected by a counting electron multiplier (Ceratron-E, Murata, Japan), and the counts are filtered by an Ortec timing-filter amplifier, and processed by a home-built data acquisition system. Singly protonated ions were produced by electrospray ionization from 1:1 water/methanol solutions containing 1% acetic acid. Precursor $(M + H)^+$ ions were accelerated to 50 keV corresponding to velocities of 1.63×10^5 to 1.70×10^5 m s^{-1}. The ions were mass-selected by a magnetic sector at mass resolution >1000 and subjected to collisions with Cs vapor in a special cell. The ion drift time through the 4 cm long collision cell was t = 234−244 ns for the fast peptide ions under study, during which time the ions underwent two collisions with Cs atoms. Radicals formed by the first collision have a Poisson distribution of drift times before being ionized by a second collision. The distribution peaks at $t/2$ = 117−122 ns, which represents the most probable radical lifetime.[11] The temperature in the cell was maintained at 105 °C, corresponding to an equilibrium Cs partial pressure of 46 mTorr and atom number density of 9×10^{12} atoms cm^{-3}. Negative ions formed in the cell were separated by kinetic energy and detected by ion counting. Multiple scans were taken and averaged to obtain sufficient ion counts for most negative ions. Spectra of $(M + H)^-$ anions from HAI were also measured with a narrow (0.1 mm) ESA entrance slit for increased kinetic energy and mass resolution.

Calculations. The conformational search for $(HAI + H)^+$ ions employed the recently developed conformational search engine which was devised to deal with protonated peptides and scan the potential energy surface (PES).[18] These calculations started with molecular dynamics (MD) simulations on the N-terminal-amino- and His-side-chain-protonated tautomers using the Insight II program (Biosym Technologies, San Diego) in conjunction with the AMBER force field.[19] During the MD we used simulated annealing techniques to produce candidate structures for further refinement, applying full geometry optimization using the AMBER force field. The AMBER optimized structures were analyzed by a conformer family search program developed in Heidelberg.[18c] This program groups optimized structures into families for which the most important characteristic torsion angles of the molecule are similar. The most stable species in the families were then fully optimized with PM3 and HF/3-21G. Forty lowest energy conformers from the above-described search in both groups of protonation tautomers were reoptimized with density functional theory calculations[20] using B3LYP/6-31+G(d,p) and including harmonic frequency analysis. These calculations were performed using the Gaussian 03 suite of programs.[21] Enthalpies and entropies were calculated using the rigid-rotor harmonic oscillator (RRHO) approximation. Although absolute enthalpies and entropies are likely to be exaggerated by RRHO due to the presence in the ions of multiple low-frequency modes, relative enthalpies and entropies were deemed to be reliable due to cancellation of errors. The fully optimized ion structures were sorted out by their relative enthalpies and free energies. Twenty-four structures of the lowest free energy group were submitted to single-point energy calculations using B3LYP and MP2 with the larger 6-311++G(2d,p) basis set of triple-ζ quality furnished with polarization and diffuse functions on all atoms. Tables of complete optimized structures are available as Supporting Information.

Radical structures were optimized with B3LYP/6-31++G(d,p) using the spin-unrestricted formalism. Local energy minima and transition states were characterized by harmonic frequency analysis to have the appropriate number of imaginary frequencies (zero for local minima and one for transition states). Improved energies were obtained by single-point calculations on the B3LYP-optimized geometries. The single-point calculations used B3LYP and Møller−Plesset perturbational theory[22] truncated at second order with valence electron only excitations (MP2(frozen core)) and the 6-311++G(2d,p) basis set. For molecular systems of the $(HAI + H)^\bullet$ radical size the larger basis set comprised 1242 primitive Gaussians. The spin-unrestricted formalism was used for calculations of open-shell systems. Contamination by higher spin states was modest, as judged from the expectation values of the spin operator $\langle S^2 \rangle$ that were ≤0.76 for UB3LYP and ≤0.78 for UMP2 calculations for most radicals. The UMP2 energies were corrected by spin annihilation[23] that reduced $\langle S^2 \rangle$ to close to the theoretical value for a pure doublet state (0.75). The single-point B3LYP and spin-projected MP2 energies were averaged (B3-PMP2),[24] which resulted in cancellation of small errors inherent to both approximations and provided dissociation and transition-state energies of improved accuracy, as has been previously shown for a number of closed-shell and open-shell systems.[25] The B3-PMP2 correction

(18) (a) Paizs, B.; Suhai, S. *Mass Spectrom. Rev.* **2005**, *24*, 508–548. (b) Paizs, B.; Suhai, S. *J. Am. Soc. Mass Spectrom.* **2004**, *15*, 103–113. (c) Paizs, B.; Suhai, S.; Hargittai, B.; Hruby, V. J.; Somogyi, A. *Int. J. Mass Spectrom.* **2002**, *219*, 203–232. (d) Wyttenbach, T.; Paizs, B.; Barran, P.; Breci, L. A.; Liu, D.; Suhai, S.; Wysocki, V. H.; Bowers, M. T. *J. Am. Chem. Soc.* **2003**, *123*, 13768–13775. (e) Polfer, N. C.; Oomens, J.; Suhai, S.; Paizs, B. *J. Am. Chem. Soc.* **2007**, *129*, 5887–5897.

(19) Case, D. A.; et al. *AMBER 99*; University of California: San Francisco, 1999.

(20) (a) Becke, A. D. *J. Chem. Phys.* **1993**, *98*, 1372–1377. (b) Becke, A. D. *J. Chem. Phys.* **1993**, *98*, 5648–5652. (c) Stephens, P. J.; Devlin, F. J.; Chabalowski, C. F.; Frisch, M. J. *J. Phys. Chem.* **1994**, *98*, 11623–11627.

(21) Frisch, M. J.; et al. *Gaussian 03*, revision B.05; Gaussian, Inc.: Pittsburgh, PA, 2003.

(22) Møller, C.; Plesset, M. S. *Phys. Rev.* **1934**, *46*, 618–622.

(23) (a) Schlegel, H. B. *J. Chem. Phys.* **1986**, *84*, 4530–4534. (b) Mayer, I. *Adv. Quantum Chem.* **1980**, *12*, 189–262.

(24) Tureček, F. *J. Phys. Chem. A* **1998**, *102*, 4703–4713.

(25) (a) Tureček, F.; Polášek, M.; Frank, A. J.; Sadílek, M. *J. Am. Chem. Soc.* **2000**, *122*, 2361–2370. (b) Polášek, M.; Tureček, F. *J. Am. Chem. Soc.* **2000**, *122*, 9511–9524. (c) Tureček, F.; Yao, C. *J. Phys. Chem. A* **2003**, *107*, 9221–9231. (d) Rablen, P. R. *J. Am. Chem. Soc.* **2000**, *122*, 357–368. (e) Rablen, P. R. *J. Org. Chem.* **2000**, *65*, 7930–7937. (f) Rablen, P. R.; Bentrup, K. H. *J. Am. Chem. Soc.* **2003**, *125*, 2142–2147. (g) Hirama, M.; Tokosumi, T.; Ishida, T.; Aihara, J. *Chem. Phys.* **2004**, *305*, 307–316.

scheme is supported by the analysis of bond dissociation in H_2, where B3LYP was found to overestimate the correlation energy while MP2 underestimated it by the same amount when compared to full-CI reference calculations.[26] Single-point energies for model imidazole ions, radicals, and transition states were also obtained by benchmark coupled-cluster calculations[27] with single, double, and disconnected triple excitations,[28] CCSD(T), using the large aug-cc-pVTZ correlation-consistent basis set.[29] These calculations are given as Supporting Information. Radical excited-state energies were calculated for optimized ion and radical geometries using time-dependent DFT with the B3LYP functional and 6-311++G(2d,p) basis set.[30] The molecular orbitals for the excited states were obtained as linear combinations of virtual orbitals using the TD-B3LYP/6-311++G(2d,p) expansion coefficients. Atomic spin and charge densities were calculated using the natural population analysis (NPA) method.[31]

Results

Peptide Radical Formation and Dissociations. Collisions of peptide cations with Cs atoms at kiloelectronvolt kinetic energies can result in electron transfer or ion excitation followed by dissociation. Both processes produce neutral intermediates, although the pertinent dissociations occur on different potential energy surfaces of the reactants. Neutral products from collision-induced ion dissociation (CID) represent a potential interference because they can be further ionized by electron transfer from Cs and give rise to anions in the $^+CR^-$ mass spectra. Fortunately, neutral products of collision-induced dissociation can be readily identified from the CID spectra that are presented together with the $^+CR^-$ spectra.

The CID/Cs spectra of $(HAI + H)^+$ ($\mathbf{1}^+$; Figure 1a) and $(HAL + H)^+$ ($\mathbf{2}^+$; Figure S1a, Supporting Information) show several standard peptide backbone fragment ions,[18a] e.g., $\mathbf{b_2}$ (*m/z* 209), $\mathbf{a_2}$ (*m/z* 181), $\mathbf{b_1}$ (*m/z* 138), and $\mathbf{a_1}$ (*m/z* 110), as well as side-chain fragments at *m/z* 283 and 284 (losses of C_4H_9 and C_4H_8) and *m/z* 82 ($C_4H_6N_2$) and products of consecutive ion dissociations, e.g., *m/z* 165 ($\mathbf{b_2} - CO_2$) and *m/z* 122 ($\mathbf{b_2} - CO_2 - C_2H_5N$). Neutral fragments of 131 Da (Ile, complementary to $\mathbf{b_2}$) and 202 Da (Ala-Ile, complementary to $\mathbf{b_1}$) are ionized by collisional deprotonation and appear as the corresponding anions in the $^+CR^-$ spectra at *m/z* 130 and 201, respectively (Figures 1b and S1b, Supporting Information). These can be denoted as $\mathbf{y_1}$ and $\mathbf{y_2}$ fragments, according to the standard nomenclature.[32]

The $^+CR^-$ spectrum of $\mathbf{1}^+$ is dominated by the survivor $(HAI + H)^-$ anion at *m/z* 340 (Figure 1b). Fragments originating from electron transfer are observed at *m/z* 338 (loss of 2H), 295 (loss of COOH), 257 (loss of the His side chain), 186 ($\mathbf{z_2}$), 115 ($\mathbf{z_1}$), and 26 (CN). The $^+CR^-$ spectrum of $\mathbf{2}^+$ (Figure S1b, Supporting Information) also shows a major peak of the reionized $(HAL + H)^-$ anion at *m/z* 340. Minor fragments appear at *m/z* 258, 257, 201, 186, 130, and 115, which are analogous to those in Figure 1b. Anions originating from **z**-type peptide fragments have been observed previously.[15c] Their stability and presence in the $^+CR^-$ spectrum are due to the positive electron affinities of C_α-carboxyl radicals and well-known stability of α-carbanions.[33] In contrast, the formation of abundant $(HAI + H)^-$ and $(HAL + H)^-$ anions is highly unusual and indicates that the intermediate radicals must have substantial electron affinities.

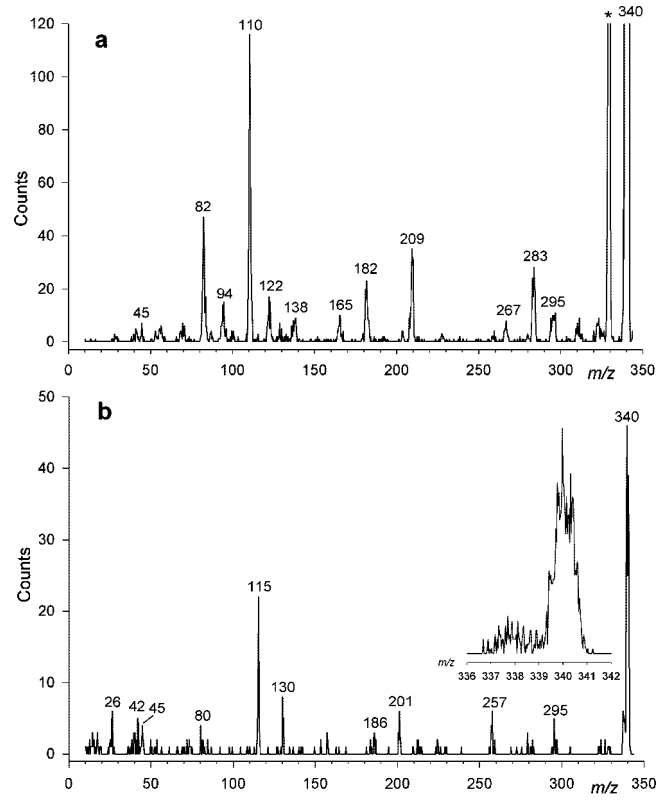

Figure 1. CID/Cs (a) and $^+CR^-$/Cs (b) mass spectra of $(HAI + H)^+$ (*m/z* 340) at a 50 keV ion kinetic energy. The asterisk in (a) indicates a precursor ion satellite reflected in the analyzer and appearing at a fractional kinetic energy.

This finding prompted us to study charge inversion in peptide ions in which the position of the His residue was varied from the N-terminus in HAL and HAAAL, through an intermediate position in AHL and AAHAL, to the C-terminus in ALH, and in which the C-terminal carboxyl was blocked as an amide (HAL-NH_2). Table 1 shows the relative intensities of (peptide + H)$^-$ anions produced by double electron transfer to (peptide + H)$^+$ precursor ions. HAI, HAL, AHL, and AAHAL showed practically identical behavior in displaying (peptide + H)$^-$ as the dominant $^+CR^-$ products. In contrast, blocking the C-terminus carboxylate in HAL-NH_2 greatly reduced the $^+CR^-$ efficiency and virtually prevented (HAL-NH_2 + H)$^-$ formation. A substantial decrease of the (peptide + H)$^-$ relative abundance was also found for ALH. HAAAL, in which the His residue and C-terminus were formally remote in the sequence, showed $(HAAAL + H)^-$ as the most abundant $^+CR^-$ product, although with a relative intensity which was lower than those for AAHAL, HAL, AHL, and HAI. These experiments indicated that the presence of a free carboxyl group in the peptide and its position with respect to the His residue were important for the

(26) Rassolov, V. A.; Ratner, M. A.; Pople, J. A. *J. Chem. Phys.* **2000**, *112*, 4014–4019.
(27) Čížek, J.; Paldus, J.; Šroubková, L. *Int. J. Quantum Chem.* **1969**, *3*, 149–167.
(28) Purvis, G. D., III.; Bartlett, R. J. *J. Chem. Phys.* **1982**, *76*, 1910–1918.
(29) (a) Dunning, T. H., Jr. *J. Chem. Phys.* **1989**, *90*, 1007–1023. (b) Woon, D. E.; Dunning, T. H., Jr. *J. Chem. Phys.* **1993**, *98*, 1358–1371.
(30) Stratmann, R. E.; Scuseria, G. E.; Frisch, M. J. *J. Chem. Phys.* **1998**, *109*, 8218–8224.
(31) Reed, A. E.; Weinstock, R. B.; Weinhold, F. *J. Chem. Phys.* **1985**, *83*, 735–745.
(32) (a) Roepstorff, P.; Fohlman, J. *Biomed. Mass Spectrom.* **1984**, *11*, 601. (b) Johnson, R. S.; Martin, S. A.; Biemann, K. *Int. J. Mass Spectrom. Ion Processes* **1988**, *86*, 137–54.
(33) (a) O'Hair, R. A. J.; Gronert, S.; DePuy, C. H.; Bowie, J. H. *J. Am. Chem. Soc.* **1989**, *111*, 3105–3106. (b) Peerboom, R. A. L.; de Koning, L. J.; Nibbering, N. M. M. *J. Am. Soc. Mass Spectrom.* **1994**, *5*, 159–68. (c) Squires, R. R. *Acc. Chem. Res.* **1992**, *25*, 461–467.

Table 1. Relative Intensities of $(M + H)^-$ Ions in the $^+CR^-$ Spectra of Histidine- and Arginine-Containing Peptides

peptide	$(M + H)^-$ relative intensity[a,b]
HAI	41 ± 3^b
HAL	46 ± 3^b
HAL-NH_2	
AHL	46 ± 3
ALH	4 ± 1
AAHAL	47 ± 2
HAAAL	31 ± 2
RAI	3 ± 1

[a] Relative to the sum of anion intensities in the $^+CR^-$ spectra. [b] One standard deviation from Poisson ion counting statistics and after reproduction of the spectra over a period of several months.

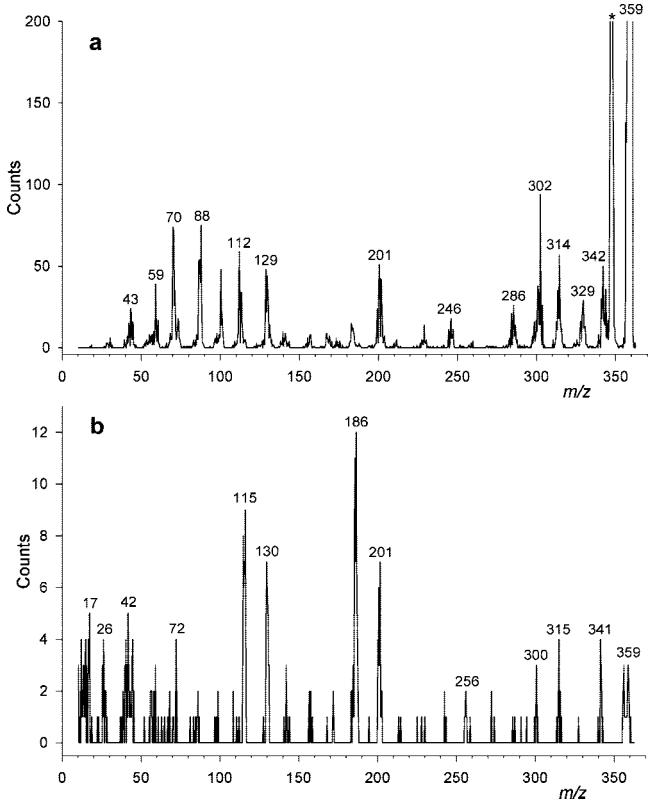

Figure 2. CID/Cs (a) and $^+CR^-$/Cs (b) mass spectra of $(RAI + H)^+$ (*m/z* 359) at a 50 keV ion kinetic energy. The asterisk in (a) indicates a reflected precursor ion satellite.

formation of $(peptide + H)^-$ upon electron transfer. As noted above, peptide radicals with structures analogous to those of their $(peptide + H)^+$ cation precursors have negative electron affinities and cannot form stable anions by capture of a second electron.[13,15] However, peptide radicals can undergo rearrangements forming intermediates that give rise to stable anions.[13,15] The reaction mechanisms for isomerizations and fragmentations of radicals will be discussed for HAI + H as a case in point in conjunction with the computational structure and energy analysis.

The CID/Cs spectrum of the arginine-containing peptide ion $(RAI + H)^+$, $\mathbf{3}^+$, Figure 2a, showed a number of fragments originating by losses of small molecules (*m/z* 342, 329, and 314) and side-chain cleavages (*m/z* 302, 100, 88, 70, and 59). Backbone $\mathbf{b_2}$ (*m/z* 228) and $\mathbf{b_1}$ (*m/z* 157) fragments were present but weak. The $^+CR^-$ spectrum of $\mathbf{3}^+$ (Figure 2b) showed a weak (3%) but reproducible survivor anion of $(RAI + H)^-$ at *m/z* 359, which indicated the presence of (RAI + H) radicals of positive electron affinity. Most of the anion signal was carried

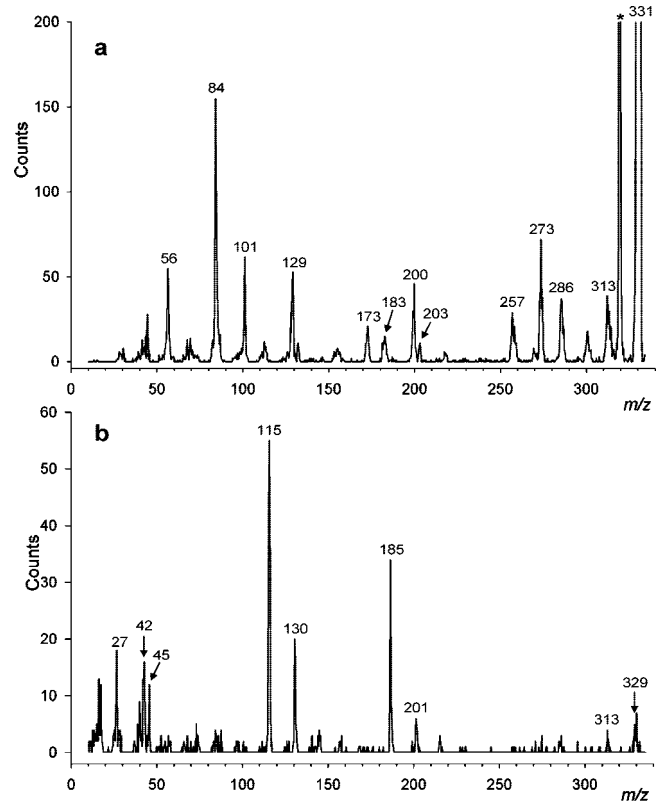

Figure 3. CID/Cs (a) and $^+CR^-$/Cs (b) mass spectra of $(KAI + H)^+$ (*m/z* 331) at a 50 keV ion kinetic energy. The asterisk in (a) indicates a reflected precursor ion satellite.

Table 2. Relative Enthalpies and Free Energies of Select $(HAI + H)^+$ Cations

	relative energy[a,b]		
	B3LYP/6−31+G(d,p)	B3-MP2/6−311++G(2d,p)	
ion	$\Delta H^\circ_{g,298}$	$\Delta H^\circ_{g,298}$	$\Delta G^\circ_{g,298}$
$\mathbf{1a}^+$	0	0	0
$\mathbf{5a}^+$	6	6	−0.7
$\mathbf{6a}^+$	15	15	12
$\mathbf{7a}^+$	7	10	12
$\mathbf{9a}^+$	15	23	20
$\mathbf{10a}^+$	18	21	18

[a] In kilojoules per mole. [b] Including zero-point energies.

by deprotonated Ala-Ile (*m/z* 201), Ile (*m/z* 130), and the $\mathbf{z_2}$ (*m/z* 186) and $\mathbf{z_1}$ (*m/z* 115) fragments. The latter two appeared at the same *m/z* as the analogous fragments from $\mathbf{1}^+$ and $\mathbf{2}^+$, confirming their assignment as C-terminal fragments. Also present were fragments at *m/z* 341 (loss of H_2O), *m/z* 315 (loss of CO_2), *m/z* 300 (loss of guanidine), and *m/z* 256 (loss of guanidine and C_4H_8) and several low-mass fragments.

The CID/Cs spectrum of the lysine-containing peptide ion $(KAI + H)^+$, $\mathbf{10}^+$, Figure 3a, showed backbone fragments, e.g., $\mathbf{b_2}$ (*m/z* 200), $\mathbf{a_2}$ (*m/z* 172), $\mathbf{b_1}$ (*m/z* 129), and $\mathbf{a_1}$ (*m/z* 101), their dissociation products at *m/z* 183 ($\mathbf{b_2} - NH_3$), *m/z* 112 ($\mathbf{b_1} - NH_3$), and *m/z* 84 ($\mathbf{a_1} - NH_3$), and fragments formed by losses of small molecules from $\mathbf{10}^+$, such as H_2O (*m/z* 313), COOH (*m/z* 286), and C_4H_9 (*m/z* 274). The $^+CR^-$ mass spectrum of $\mathbf{10}^+$ did not display a survivor anion at *m/z* 331 (Figure 3b). The major fragments in the $^+CR^-$ spectrum were the $\mathbf{z_2}$ (*m/z* 186) and $\mathbf{z_1}$ (*m/z* 115) anions, which were accompanied by deprotonated Ala-Ile (*m/z* 201) and Ala (*m/z* 130) from

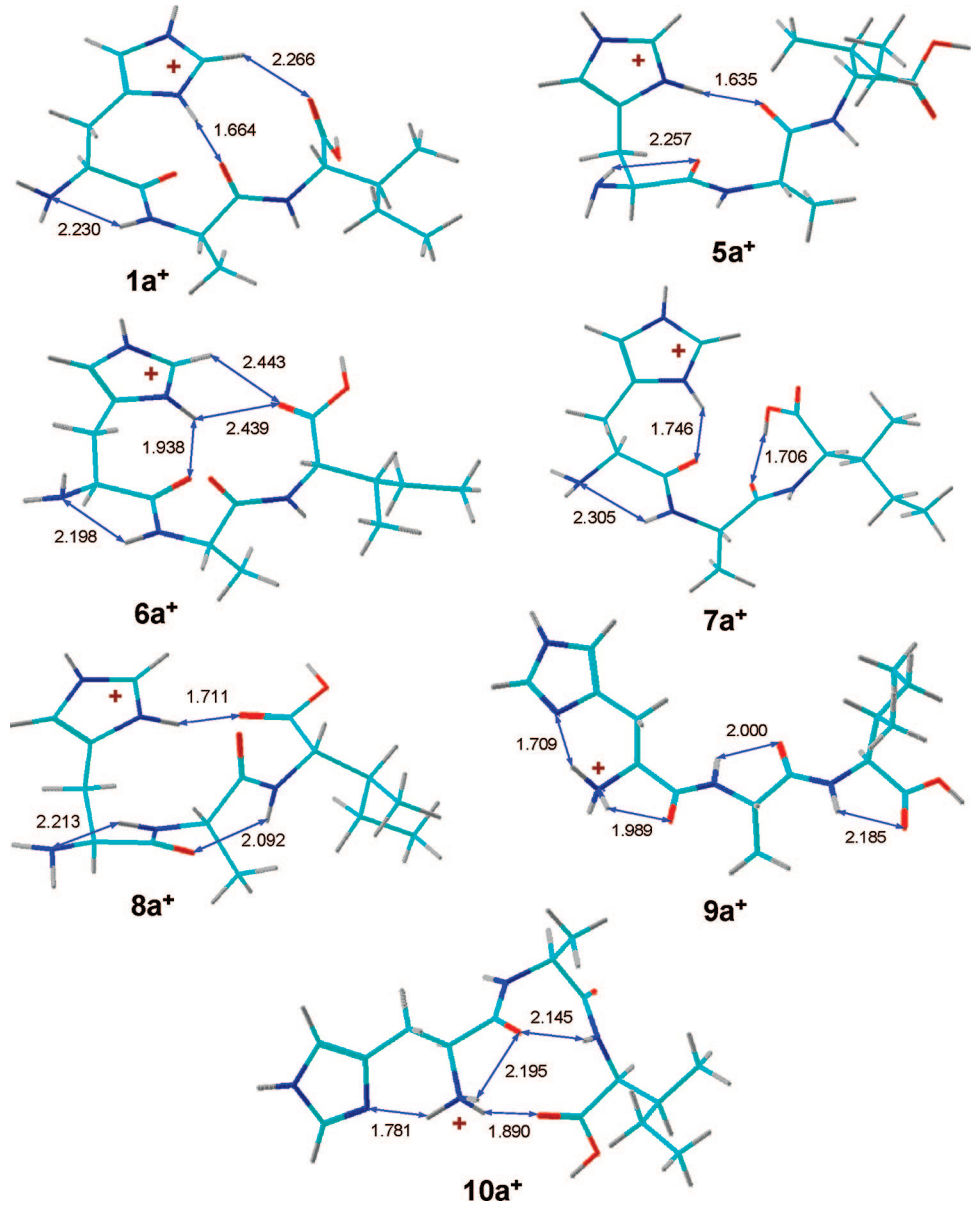

Figure 4. B3LYP/6-31+G(d,p)-optimized structures of $\mathbf{1}^+-\mathbf{10a}^+$. The atom color coding is as follows: turquoise, C; red, O; blue, N; gray, H. The blue double-ended arrows indicate hydrogen bonds. The distances are given in angstroms.

reionization of the respective products of collision-induced ion dissociations (vide supra).

In summary, the $^+CR^-$ spectra of $\mathbf{1}^+-\mathbf{10}^+$ indicated that the formation of nondissociating $(peptide + H)^-$ anions was *amino acid specific*, with the strongest stabilizing effect being due to the His residue and a weaker one to the Arg residue, while no stabilization was observed for the Lys residue. Moreover, the presence in the peptide of a free carboxyl and its position relative to the His residue were important. The rationale for stabilization of the pertinent peptide + H radicals and anions was sought through a detailed structure analysis of the HAI + H system, as described next.

Cation Structures. Protonation of HAI may occur at the N-terminal amino group or in the histidine imidazole ring, which are the two presumably most basic sites in the peptide. Both groups were investigated, and the His-protonated structures were found to be the lowest energy and free energy isomers. B3LYP/6-31+G(d,p)-optimized structures of His-protonated $(HAI + H)^+$ conformers are represented by five types (**1**, **5**, **6**, **7**, **8**) that differ in the intramolecular H-bonding patterns. Each type further encompasses multiple rotamers differing in the conformations of the isoleucine *sec*-butyl and COOH groups, e.g., $\mathbf{1a}^+-\mathbf{1m}^+$, $\mathbf{5a}^+-\mathbf{5h}^+$, etc. The lowest energy conformers in each group are given in Table 2; a complete list is given in Table S1 (Supporting Information). Ion and radical structures shown in the schemes and figures use the following atom color coding: turquoise, C; gray, H; red, O; blue, N. Types **1** and **5**, represented by structures $\mathbf{1a}^+$ and $\mathbf{5a}^+$ (Figure 4), are the thermodynamically most stable conformers by combined B3LYP and MP2/6-311++G(2d,p) energy calculations. Both $\mathbf{1a}^+$ and $\mathbf{5a}^+$ involve tight hydrogen bonding between the protonated imidazole ring and the Ala amide carbonyl, which allows for a favorably large N−H···O angle (173−176°, Figure 4). Ions $\mathbf{1a}^+$ and $\mathbf{5a}^+$ differ in the conformation about the His amide bond, which allows for H-bonding of the amide proton in $\mathbf{1a}^+$ and one of the N-terminal amine hydrogens in $\mathbf{5a}^+$. Several less stable conformer structures of the $\mathbf{1}^+$ and $\mathbf{5}^+$ types are shown in Figure S2 (Supporting Information). Ions of the $\mathbf{1}^+$

Table 3. Ion Recombination Energies and Radical Electron Affinities

radical/ion		energy[a,b] B3LYP/6-31++G(d,p)	energy[a,b] B3-PMP2/6-311++G(2d,p)
1a → **1a**$^+$	RE_a	330	315 (3.27)[c]
	RE_v		221 (2.29)
5a → **5a**$^+$	RE_a	333	317 (3.28)
	RE_v		227 (2.35)
5c → **5c**$^+$	RE_a	329	312 (3.23)
	RE_v		225 (2.33)
5d → **5d**$^+$	RE_a	333	315 (3.27)
	RE_v		227 (2.35)
6a → **6a**$^+$	RE_a	357	338 (3.51)
	RE_v		234 (2.42)
7a → **7a**$^+$	RE_a	347	333 (3.45)
	RE_v		230 (2.39)
9a → **9a**$^+$	RE_a	278	262 (2.72)
	RE_v	250	*d*
10a → **10a**$^+$	RE_a	304	290 (3.00)
	RE_v	243	*d*
1a$^-$ → **1a**	EA_v	−39	−36 (−0.38)
5a$^-$ → **5a**	EA_v	−61	−61 (−0.63)
11$^-$ → **11**	EA_a	202	213 (2.21)
	EA_v	41	50 (0.51)
12$^-$ → **12**	EA_a	246	250 (2.59)
	EA_v		130 (1.35)
16$^-$ → **16**	EA_v		83 (0.86)
18$^-$ → **18**	EA_v		36 (0.37)
z$_1$	EA_a	157	156 (1.61)
	EA_v		126 (1.31)
z$_2$	EA_a	136	137 (1.42)
	EA_v		96 (0.99)

[a] In units of kilojoules per mole unless stated otherwise. [b] RE_a and EA_a are absolute values of adiabatic ion recombination energies or radical electron affinities, respectively, including B3LYP/6-31++G(d,p) zero-point corrections. RE_v and EA_v are absolute values of the respective vertical recombination energies or electron affinities. The vertical energies do not include zero-point corrections. [c] Values in parentheses are in electronvolts. [d] The UMP2/6-311++G(2d,p) single-point calculations failed to converge.

and **5**$^+$ types are estimated to amount to, respectively, 39% and 60% of the equilibrium population of $(HAI + H)^+$ gas-phase ions at 298 K. Types **6** (**6a**$^+$), **7** (**7a**$^+$), and **8** (**8a**$^+$) (Figure 4) are minor conformers that are estimated to be populated at <0.2% each.

N-terminus-protonated tautomers are represented by the lowest energy structures **9a**$^+$ and **10a**$^+$ (Figure 4), each also having an Ile side-chain rotamer of a comparable relative energy (**9b**$^+$ and **10b**$^+$, respectively). However, according to the calculated $\Delta G°_{g,298}$, ions **9a**$^+$ and **10a**$^+$ are 20 and 18 kJ mol^{-1}, respectively, less stable than **1a**$^+$, and are not expected to be significantly populated in the gas-phase equilibrium mixture. Consistent with this conclusion, the $^+CR^-$ spectrum of $(HAI + H)^+$ shows negligible loss of ammonia (*m*/*z* 323), which would be expected to be the dominant dissociation of radicals formed from **9**- and **10**-type ions having N-terminal NH_3 groups.[8,15,34]

Electron Transfer. Electron attachment was studied computationally for **1a**$^+$, **5a**$^+$, **5c**$^+$, **5d**$^+$, **6a**$^+$, **7a**$^+$, **9a**$^+$, and **10a**$^+$. The calculated vertical recombination energies for **1a**$^+$, **5a**$^+$, **5c**$^+$, **5d**$^+$, **6a**$^+$, and **7a**$^+$ are in the range of 2.29−2.42 eV. The adiabatic recombination energies of **9a**$^+$ and **10a**$^+$ are 2.72 and 3.00 eV, respectively. The different RE values for these N-terminal ammonium ions are due to the unique electronic structure of radical **10a**, as discussed later. In general, the recombination energies of all $(HAI + H)^+$ ions are smaller than the ionization energy of Cs (3.894 eV), implying that collisional electron transfer from Cs is *endoergic* regardless of the peptide ion secondary structure. A common feature of electron attachment to His-protonated $(HAI + H)^+$ ions is the large differences in the vertical and adiabatic recombination energies (Table 3), which indicate large Franck−Condon effects in collisional electron transfer. From the $|RE_a - RE_v|$ differences and including the rovibrational enthalpy of the precursor ions (52 kJ mol^{-1} at 298 K),[35] we estimate the mean vibrational excitation in **1a**, **5a**, **5c**, **5d**, **6a**, and **7a** radicals to be in the range of 130−140 kJ mol^{-1}. The large Franck−Condon effects are mainly caused by differences in the equilibrium geometries of the protonated His imidazole ring in the cations and radicals (Figure S3, Supporting Information). Compared to the cations, the histidine radicals show longer C−N bonds and have puckered imidazole rings (Figure S3, Supporting Information). These changes upon electron attachment are analogous to those in protonated imidazole.[36] The other major difference between the ion and radical equilibrium structures is the different N−H···O hydrogen bond lengths, which are extended by 0.3 Å in the radicals, indicating hydrogen bond weakening upon electron attachment.

Table 4. Radical Relative, Transition-State, and Dissociation Energies

radical/reaction	relative energy[a,b] B3LYP/6-31++G(d,p)	relative energy[a,b] B3-PMP2/6-311++G(2d,p)
1a	0.0	0.0
1a → **5a**	0.9	4.1
1a → **5d**	7.0	9.8
1a → **6a**	−12	−7.9
1a → **5c**	12	14
1a → **7a**	−10	−6.1
1a → **9a**	67	76
1a → **10a**	44	45
1a → TS1	−2	−4
1a → **11**	−77	−67
5a → TS2	−8	−13
5a → **12**	−12	−10
5a → TS3	66	68
5a → **15**	−27	−24
5a → **18** + CO_2	19	16
5a → TS6	71	66
5a → **14**	3	−3
5a → **c$_1$** + **z$_2$**	8	20
5a → **c$_2$** + **z$_1$**	−6	8
z$_2$ → **z$_1$** + C_3H_3NO[c]	187	207
9a → **16** + NH_3	−149	−144
9a → TS4	−4	2.4
9a → **17** + H	−8	−31
9a → TS5	3	0.3

[a] In kilojoules per mole. [b] Including B3LYP/6-31++G(d,p) zero-point vibrational energies and referring to 0 K. [c] Alanine α-lactam.

Radicals. Radicals **1a**, **5a**, **5c**, **5d**, **6a**, **7a**, **9a**, and **10a** were calculated to be potential energy minima. In contrast to the order of ion relative energies, **6a** is the most stable structure among the His-protonated radicals, followed by **7a** and **1a** (Table 4). However, the energy differences among the radicals are small,

(34) (a) Chakraborty, T.; Holm, A. I. S.; Hvelplund, P.; Nielsen, S.; Brøndsted; Poully, J.-C.; Worm, E. S.; Williams, E. R. *J. Am. Soc. Mass Spectrom.* **2006**, *17*, 1675–1680. (b) Holm, A. I. S.; Hvelplund, P.; Kadhane, U.; Larsen, M. K.; Liu, B.; Nielsen, S.; Brøndsted; Panja, S.; Pedersen, J. M.; Skrydstrup, T.; Støchkel, K.; Williams, E. R.; Worm, E. S. *J. Phys. Chem. A* **2007**, *111*, 9641–9643.

(35) (a) Wolken, J. K.; Tureček, F. *J. Phys. Chem. A* **1999**, *103*, 6268–6281. (b) Tureček, F. *Int. J. Mass Spectrom.* **2003**, *227*, 327–338.

(36) Nguyen, V. Q.; Tureček, F. *J. Mass Spectrom.* **1996**, *31*, 1173–1184.

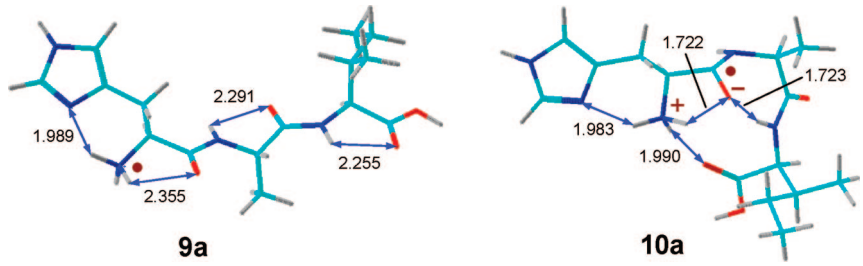

Figure 5. B3LYP/6-31++G(d,p)-optimized structures of radicals **9a** and **10a**. The geometry description is as in Figure 4.

Scheme 2

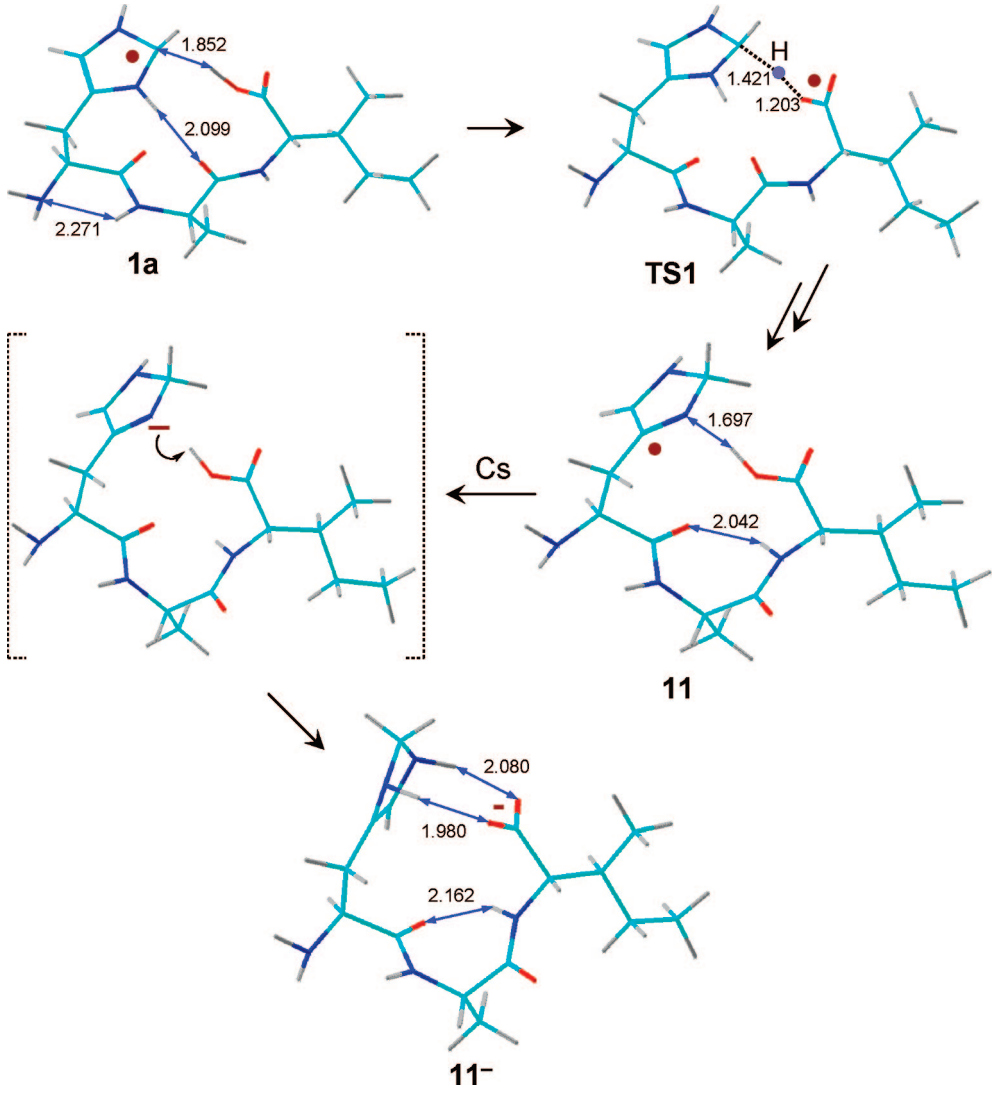

and because of weakened H-bonding and substantial vibrational excitation upon electron attachment (vide supra), the radical conformers may rapidly interconvert. Radicals **9a** and **10a** are less stable than **1a**−**7a**, and their structures, electronic properties, and dissociations will be discussed only briefly.

Radical **1a** has the COOH group in proximity of the imidazole ring (Scheme 2). This radical conformer is calculated to undergo extremely facile migration of the carboxyl hydrogen atom onto C-2 of the imidazole ring. The transition-state (TS1) energy for the migration, $E_{TS1} = -4$ kJ mol^{-1} relative to **1a**, indicates that **1a** is metastable with respect to isomerization. The negative value of E_{TS1} originates from the decrease of the zero-point energy due to loss of the O−H stretching mode in the transition state. The incipient COO radical from isomerization through TS1 is not a local energy minimum and upon conformational reorganization exothermically abstracts a H atom from the proximate imidazole N−H bond to re-form the COOH group. The net result of this sequence is an exothermic isomerization of the imidazole radical in **1a** to the more stable (2*H*)-imidazoline radical structure **11**. It should be noted that

(37) The barrier for 1,2-hydrogen N-1 → C-2 migration in the imidazolium radical is calculated as $E_{TS} = 150$ kJ mol^{-1} by B3-PMP2/6-311++G(2d,p) + ZPVE corrections, in good agreement with the CCSD(T)/aug-cc-pVTZ + ZPVE value of 151 kJ mol^{-1}.

Scheme 3

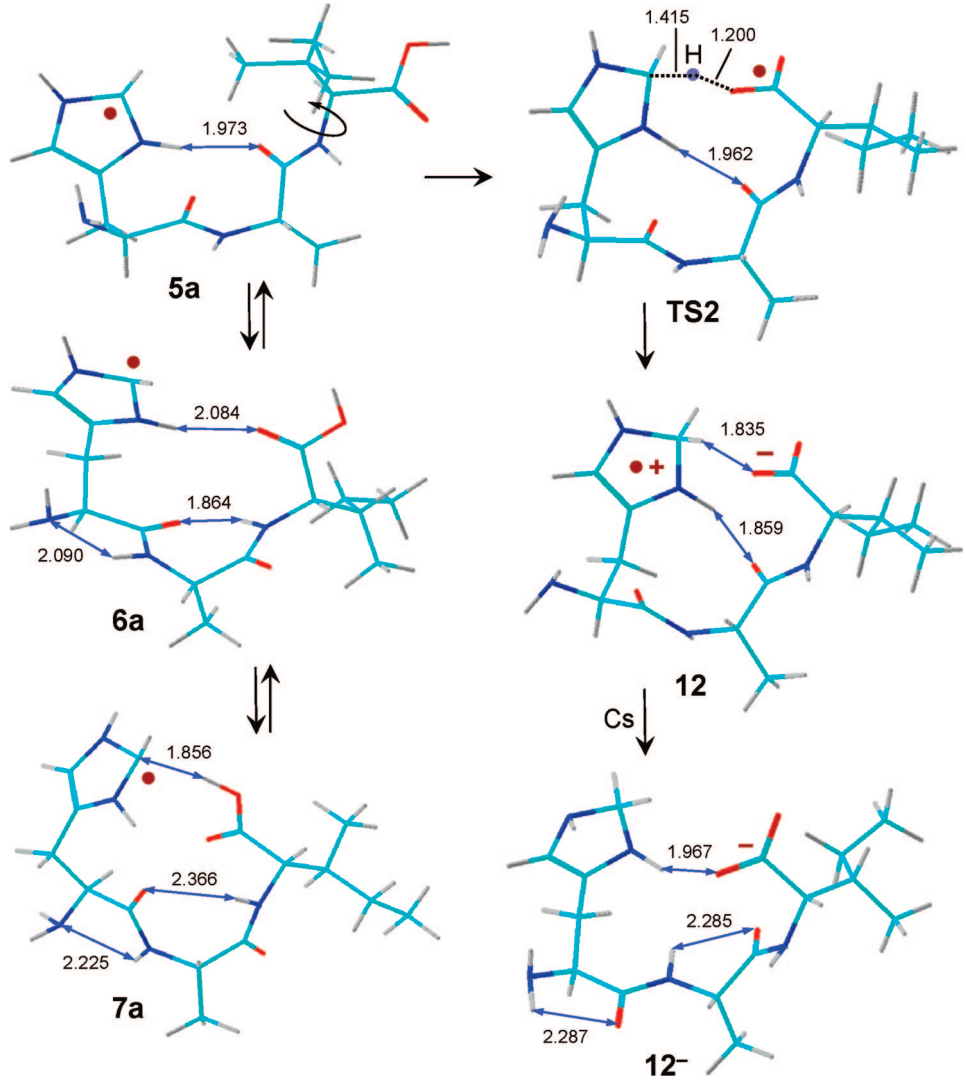

unassisted 1,2-H atom migrations in simple imidazole radicals, albeit exothermic, face substantial activation energies.[36,37] The practically barrierless **1a** → **11** isomerization can be attributed to the relay effect of the carboxyl group, which catalyzes transport of the hydrogen atom between the imidazole N and C atoms. Similar "catalyzed" hydrogen atoms transfers have been reported for gas-phase ions.[38] However, their occurrence in neutral radicals appears to be less common and may be conditioned upon similar hydrogen atom affinities of the involved functional groups or other electronic effects, as discussed below.

Facile carboxylate H atom transfer was also calculated to occur in **5a**, where it had $E_{TS2} = -13$ kJ mol^{-1} (Table 3). In contrast to **1a**, H atom migration in **5a** forms a carboxylate radical intermediate (**12**, Scheme 3) which is a local energy minimum. The fact that the potential energy of TS2 is below those of both **5a** and **12** is again due to zero-point vibrational energy effects. The existence of the COO radical **12** can be attributed to its unusual electronic structure (see below) and conformational effects that prevent the proximate N−H bond from being directly accessible for reverse H atom transfer because of hydrogen bonding to the Ala amide carbonyl. Given the vibrational excitation in vertically formed **5a**, one can presume that intermediate **12** is likely to undergo conformational transformations that would bring the N−H bond close to the COO group to trigger exothermic H atom transfer and isomerization in the imidazole ring. Interestingly, loss of CO_2 is only a minor dissociation upon $^{+}CR^{-}$ of $(HAI + H)^{+}$ ions and evidently does not compete with other rearrangements in the intermediate radicals.

Radical isomers **9a** and **10a** are less stable than **1a**−**7a** (Table 4) and, considering the low population of type $\mathbf{9}^{+}$ and $\mathbf{10}^{+}$ cations, are unlikely to play an important role in $^{+}CR^{-}$ dissociations of HAI + H radicals. Nevertheless, the structure motifs in **9a** and **10a**, such as the N-protonated terminus with H bonds to the proximate functional groups, may appear in other His-terminated peptides, and since **9a** and **10a** show some interesting structures and electronic properties, they are worth briefly mentioning here. Structure **9a** (Figure 5) is a typical hypervalent ammonium radical, as evidenced by both its electronic structure and predicted dissociation pathways. The SOMO in **9a** has a 3s Rydberg-like orbital as the main component which is localized about the ammonium group

(38) (a) Tureček, F.; Drinkwater, D. E.; McLafferty, F. W. *J. Am. Chem. Soc.* **1990**, *112*, 993–997. (b) Bohme, D. K. *Int. J. Mass Spectrom. Ion Processes* **1992**, *115*, 95–110. (c) Audier, H. E.; Mourgues, P.; van der Rest, G.; Chamot-Rooke, J.; Nedev, H. *Adv. Mass Spectrom.* **2001**, *15*, 101–121.

Scheme 4

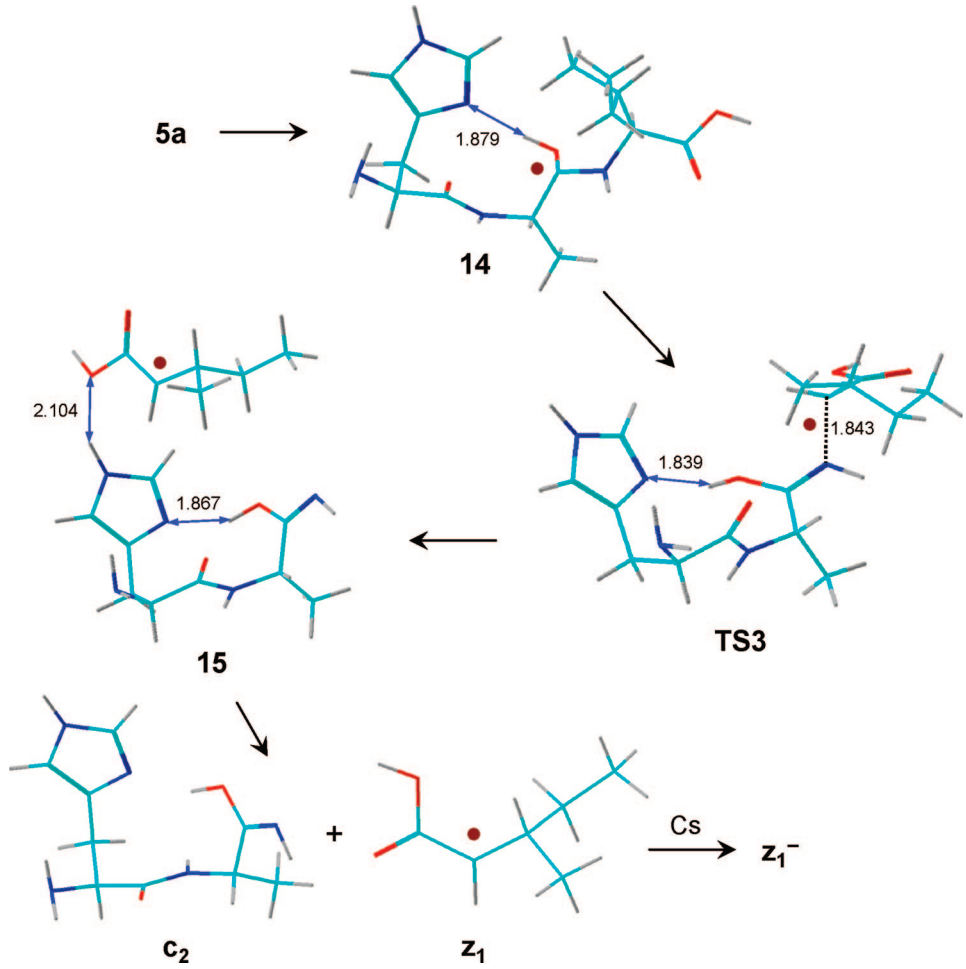

(Figure S4, Supporting Information). The low-lying A and B states are carboxyl and amide π^* orbitals, respectively, which can be viewed as zwitterionic states with a positively charged ammonium group and negatively charged hydroxy or aminoketyl anion radicals.

The other N-terminus-protonated radical (**10a**) is 31 kJ mol^{-1} more stable than **9a**. Rather unexpectedly, **10a** is calculated to be a zwitterion in its ground electronic state. This is evidenced by the fact that the His amide group is 32.5° pyramidized at the carbonyl C atom and has a long C−O bond (1.327 Å) (Figure 5). The SOMO in **10a** is an aminoketyl π orbital which is contained within the His amide group (Figure S5, Supporting Information). The latter accounts for 89% of atomic spin density and carries −0.81 negative charge at the CONH atoms. In contrast, the N-terminal ammonium group carries only 4% of atomic spin density and has a +0.56 positive charge. The unusual structure of **10a** can be explained by stabilization by hydrogen bonding of both the cationic ammonium and anionic aminoketyl groups. The Figure 5 structures show that there is efficient internal solvation of the NH_3 group by H bonding to the imidazole imine and the amide and carboxyl C=O groups. Likewise, the aminoketyl oxygen is H bonded to protons of the N-terminal ammonium and Ala amide groups. Obviously, this H-bonding pattern is absent in **9a**, which prefers an ammonium radical structure in the ground electronic state.

Vertical electron attachment to radicals **1a** and **5a** was calculated to be 40−60 kJ mol^{-1} *endothermic*, indicating negative electron affinities for the radicals (Table 3). Hence, **1a** and **5a** cannot form valence-bound anions. The calculated energies further indicate that in spite of moderate dipole moments in **1a** and **5a** (calculated as 5.6 and 3.0 D, respectively) even dipole-bound anions[39] are likely to be unstable. In light of the intrinsic instability of **1a**$^-$ and **5a**$^-$, the formation of stable anions upon $^+CR^-$ can only occur through intermediates such as **11** and **12**, which both have positive vertical electron affinities (Table 3). Note that while the carboxylate anion **12**$^-$ is a potential energy minimum (Scheme 3), the imidazolide anion **11**$^-$ is calculated to undergo spontaneous proton transfer from the COOH group to the imidazole imide nitrogen to form the very stable carboxylate anion **13**$^-$ (Scheme 2). The difference in energy between the conformational isomers **12**$^-$ and **13**$^-$ (21 kJ mol^{-1}) can be ascribed to the stabilizing H bonding between the COO^- group and both imidazole N−H bonds in the latter conformer.

Peptide Radical Dissociations. In addition to the major fraction of surviving $(HAI + H)^-$ and $(HAL + H)^-$ anions, the $^+CR^-$ spectra also show $\mathbf{z_1}$ and $\mathbf{z_2}$ anion fragments (Figures 1b and S1b, Supporting Information), which are produced by collisional reionization of the corresponding $\mathbf{z_1}$ and $\mathbf{z_2}$ radicals. These are C_α radicals that arise by N−C_α bond dissociations and have substantial positive electron affinities, both vertical and adiabatic (Table 3). Interestingly, the $\mathbf{z_1}$ fragment anion, which is more

(39) (a) Jordan, K. D. *Acc. Chem. Res.* **1979**, *12*, 36–42. (b) Simons, J. Anions. In *The Encyclopedia of Mass Spectrometry*; Armentrout, P. B., Ed.; Elsevier: Amsterdam, 2003; Vol. 1, Chapter 2, pp 55−68.

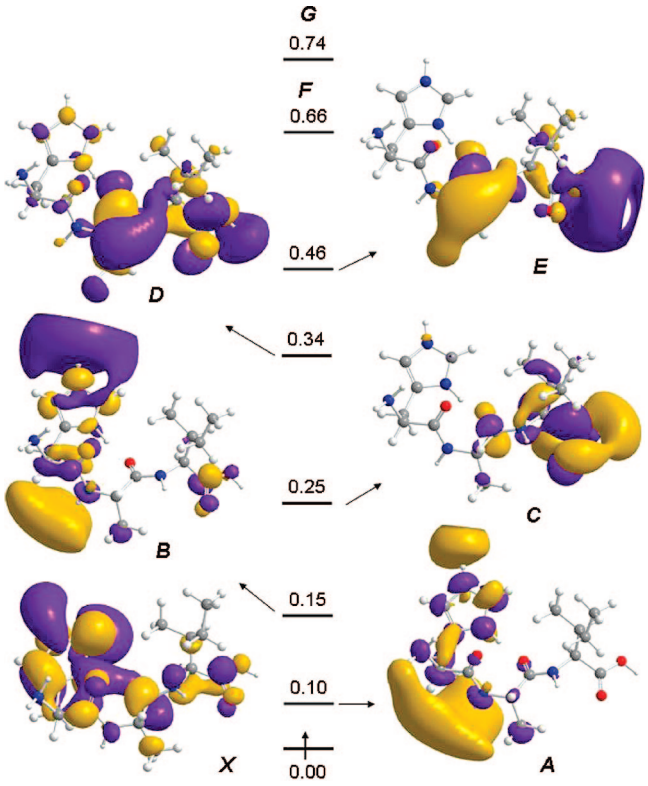

Figure 6. Excited electronic states in vertically formed **5a**. The relative excitation energies from TD-B3LYP/6-311++G(2d,p) calculations are in electronvolts.

abundant in the $^{+}CR^{-}$ spectrum, corresponds to the C_{α}-carboxyl radical, which has a greater electron affinity than the C_{α}-amide radical $\mathbf{z_2}$ (Table 3). The formation of the $\mathbf{z_1}$ and $\mathbf{z_2}$ radicals can be visualized by N−C_{α} bond cleavage in HAI + H and HAL + H radicals. The energetics of this bond dissociation was studied for the former system according to the previously suggested mechanisms.[2a,b,7]

The formation of the $\mathbf{c_1} + \mathbf{z_2}$ fragment pair is 20 kJ mol^{-1} endothermic relative to **5a**, as calculated for an enol−imine tautomer of $\mathbf{c_1}$. The formation of the $\mathbf{c_2} + \mathbf{z_1}$ fragment pair is only 8 kJ mol^{-1} endothermic, and thus, the latter fragments are slightly more favorable by their threshold energy. The formation from **5a** of the $\mathbf{c_2} + \mathbf{z_1}$ fragments can be visualized in three steps (Scheme 4). The first is an imidazole proton migration onto the Ala amide carbonyl to give intermediate aminoketyl radical **14**, which is nearly isoenergetic with **5a** (Table 4). The TS energy for the migration has not been determined for **5a**, but can be estimated to be close to 70 kJ mol^{-1} from studies of similar histidine radical systems.[40] N−C_{α} bond cleavage in **14** overcomes a barrier of 72 kJ mol^{-1} in TS3 (68 kJ mol^{-1} relative to **5a**, Table 4) to form a dipole−dipole complex (**15**) which is 24 kJ mol^{-1} more stable than **5a** (Table 4). Fragment separation in **15** is expected to require no barrier above the thermochemical threshold. The calculated TS energies indicate that although the energy barriers to His H atom migration and N−C_{α} bond cleavage are relatively moderate in HAI + H radicals, they are substantially greater than the barrier for the inverse and exothermic migration of the COOH hydrogen atom to the imidazole ring. It therefore appears unlikely that the three-step N−C_{α} bond cleavage shown in Scheme 4 could be competitive with the imidazole isomerization on the potential energy surface of the ground electronic state.

The N−C_{α} bond dissociations upon electron transfer can be visualized as proceeding from low-lying excited states (e.g., B, C, and D in **1a** and C and D in **5a**, Figure 6) when accessed by electron transfer. These states show substantial electron density in the π^* orbital of the Ala amide group, indicating that the amide oxygen can exothermically abstract an imidazole proton according to the amide superbase mechanism.[41] Alternatively, the π^* electronic states may undergo N−C_{α} bond cleavage triggered by the unpaired electron density in the amide group. Thus, the formation of the $\mathbf{c_2} + \mathbf{z_1}$ neutral fragments is more compatible with the electronic properties of excited states in the HAI + H radicals than with those of the ground states.

We note that a consecutive dissociation, $\mathbf{z_2} \rightarrow \mathbf{z_1} + C_3H_5NO$, was calculated to require a prohibitively high threshold energy for the formation of alanine α-lactam as the C_3H_5NO fragment ($\Delta H_{rxn} = 207$ kJ mol^{-1}, Table 4). In addition, the dissociation of the N−C_{α} bond in the $\mathbf{z_2}$ radical showed an additional >20 kJ mol^{-1} barrier along the reaction coordinate above the thermochemical threshold. Such energies are not readily available to HAI + H radicals formed by electron transfer from Cs, which is estimated to result in 130−140 kJ mol^{-1} vibrational excitation (vide supra). Hence, we conclude that the $\mathbf{z_2}$ and $\mathbf{z_1}$ fragments are formed by competitive dissociations of the pertinent N−C_{α} bonds in **1a** or **5a**. The greater relative abundance of the $\mathbf{z_1}$ anions is presumably due to the more favorable kinetics and thermochemistry for the $\mathbf{z_1}$ radical formation and its higher electron affinity.

Losses of NH_3 and CO_2 are some other common dissociations of peptide cations upon electron capture or transfer.[2c] However, the $^{+}CR^{-}$ spectra of $(HAI + H)^{+}$ and $(HAL + H)^{+}$ show very minor losses of small molecules. Radical **9a** in its X state is predicted to undergo extremely facile and practically barrierless loss of ammonia through TS4 ($E_{TS4} = 2.4$ kJ mol^{-1}) to exothermically form His C_{α} radical **16** (Scheme 5, Table 4). The virtual absence of NH_3 loss in the $^{+}CR^{-}$ spectrum is consistent with the negligible population of N-terminus-protonated radical tautomers, as predicted by our conformation analysis of precursor ion populations. Note that the $(MH - NH_3)^{\bullet}$ fragment (**16**) from **9a** has a positive electron affinity (Table 3), and if formed, it should be detectable as a negative ion. Loss of an ammonium H atom from **9a** requires an activation energy of only 0.3 kJ mol^{-1} in TS5 (Table 4) to exothermically form neutral HAI peptide conformer **17** at −31 kJ mol^{-1} relative to **9a**. Our experiments did not establish which H atoms were lost upon $^{+}CR^{-}$ of **1a** or **5a**, so this minor point remains unresolved.

Loss of CO_2 is possible from intermediate **12**, which has a COO group (Scheme S1, Supporting Information). The calculated C_{α}−COO dissociation energy in **12**, forming **18** (25 kJ mol^{-1}, Table 4), indicates that the radical intermediate is only marginally stable. However, dissociation of the C_{α}−COO bond in **12** must overcome a substantial barrier in TS6 (66 kJ mol^{-1}, Table 4), which disfavors the loss of CO_2 against the exothermic $\mathbf{12} \rightarrow \mathbf{11}$ isomerization. The kinetic stability of **12** with respect to CO_2 loss is outstanding when compared with that of decarboxylations of amino acid COO radicals which are highly

(40) The analogous N−H → O=C migration in histidine *N*-methylamide radical was calculated to have $E_{TS} = 64$ kJ mol^{-1}.

(41) Syrstad, E. A.; Tureček, F. *J. Am. Soc. Mass Spectrom.* **2005**, *16*, 208–224.

Scheme 5

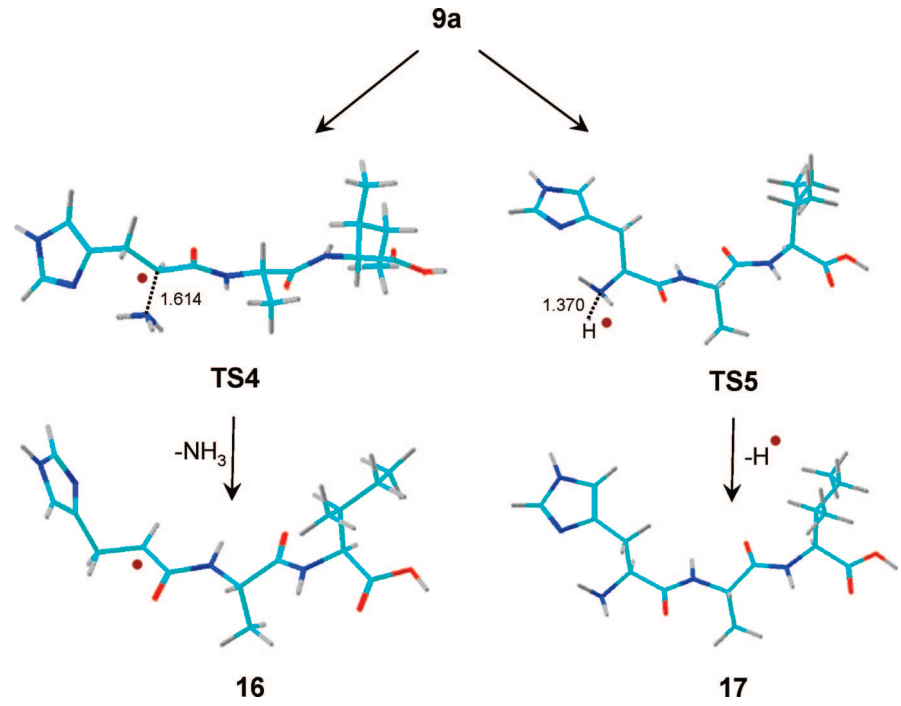

Scheme 6

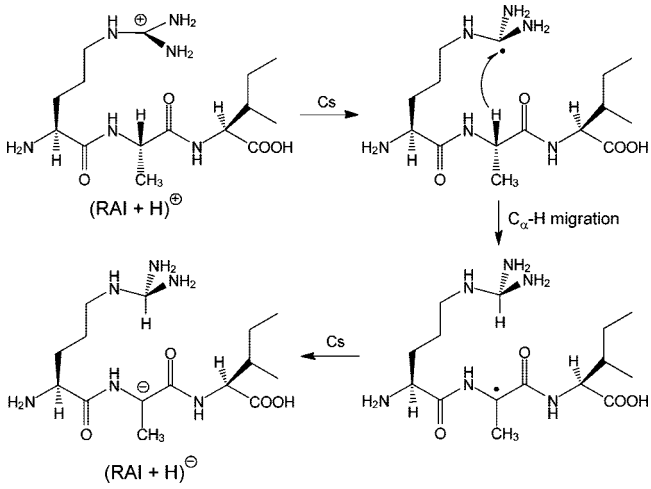

exothermic.[42] The stability of **12** can be attributed to its unusual electronic properties, as discussed below.

RAI + H Radicals. The minor fraction of surviving RAI + H anions in the $^{+}CR^{-}$ spectra is consistent with inverse migrations of C_α H atoms to the guanidine group in arginine radicals, as reported recently.[11−13] These have been shown to be exothermic and have low activation energies in arginine radicals formed by charge reduction. C_α radical intermediates produce stable anions upon collisional electron transfer from alkali-metal atoms.[13,14] Scheme 6 depicts a rearrangement in $(RAI + H)^{\bullet}$ involving the Ala C_α H atom. Calculations on the RAI + H radicals including conformational analysis of precursor ions would be necessary to describe the mechanistic details, energetics, and kinetics of inverse arginine rearrangements in RAI + H radicals, which are beyond the scope of this study.

Discussion

The experimental data point to an unusual formation of major stable anions upon double electron transfer to $(HAI + H)^+$, $(HAL + H)^+$, $(AHL + H)^+$, $(HAAAL + H)^+$, and $(AAHAL + H)^+$ ions and, to a smaller extent, $(ALH + H)^+$ and $(RAI + H)^+$ ions. In contrast, HAL-NH_2 in which the carboxyl group was absent did not produce stable anions. The experimental data are explained by hidden hydrogen migrations in His-containing radical intermediates involving the carboxyl group, which catalyzes isomerization of the original imidazolium structures to more stable imidazoline ones. We emphasize that this interpretation is not obvious and cannot be predicted on the grounds of analyzing the properties of separate imidazole and carboxylate radicals. For example, the O−H bond dissociation energy in carboxylic acids, e.g., glycine and acetic acid, has been calculated as 472 and 464 kJ mol^{-1}, respectively.[43−46] These bond dissociation energies are substantially higher than the hydrogen atom affinities of imidazole radicals,[36] which we calculate as 342 and 381 kJ mol^{-1} for the C-2 and C-5 positions, respectively (CCSD(T)/aug-cc-pVTZ + ZPVE energies, Table S2, Supporting Information). Thus, hydrogen atom transfer from a COOH group to an isolated imidazole radical is quite endothermic. This is contrasted by the *exothermic* hydrogen migrations in **1a** and **5a**, which form transient (2*H*)-imidazoline intermediates, e.g., **12**. The stabilization of these intermediates, as well as of the connecting transition states TS1 and TS2, is

(42) (a) Yu, D.; Rauk, A.; Armstrong, D. A. *J. Am. Chem. Soc.* **1995**, *117*, 1789–1796. (b) Armstrong, D. A.; Rauk, A.; Yu, D. *J. Chem. Soc., Perkin Trans.* **1995**, *2*, 553–560.

(43) From the estimated heats of formation (kJ mol^{-1}) of H_2NCH_2COO radical (−138),[42] H (218), and gaseous glycine (−394).[44]

(44) Pedley, J. B.; Naylor, R. D.; Kirby, S. P. *Thermochemical Data of Organic Compounds*, 2nd ed.; Chapman and Hall: London, 1986; pp 233−617.

(45) From the heats of formation (kJ mol^{-1}) of CH_3COOH (−432)[44] and CH_3COO radical (−181).[46]

(46) De Smedt, F.; Bui, X. V.; Nguyen, T. L.; Peeters, J.; Vereecken, L. *J. Phys. Chem. A* **2005**, *109*, 2401–2409.

due to polarization of the (2*H*)-imidazoline and carboxylate groups. NPA population analysis of electron distribution in **12** indicates 95% of unpaired electron density to be localized within the formally closed-shell imidazoline ring whereas the COO group accounts for only 4%. Conversely, the atomic charge densities place a +0.81 charge in the imidazoline ring and −0.75 charge in the COO group. These spin and charge distributions point to a zwitterionic electronic structure comprising an imidazoline cation radical which forms a salt bridge to a carboxylate anion. To our knowledge, this is the first case of an intrinsically stable open-shell salt bridge structure in peptides. The remarkable stability of this structure hinges on strong dipolar interactions, whose magnitude can be estimated as follows. The ionization energy of an isolated imidazoline system is calculated as 6.20 eV for 4-methyl-(2*H*)-imidazoline, which is analogous to that of the His side chain in **12**. The electron affinity of a COO group is estimated from that of the glycine COO radical as 3.35 eV.[47] Thus, in the absence of a stabilizing dipolar interaction, electron transfer from the imidazoline ring to the COO moiety would be 6.20 − 3.35 = 2.85 eV (275 kJ mol^{-1}) endothermic. This implies that the [imidazoline]$^{\bullet+}\cdots{}^{-}$OOC structure in **12** owes its stability to substantial dipolar stabilization on the order of 285 kJ mol^{-1} to account for both the charge transfer and exothermic **5** → **12** isomerization.[48]

The detection of stable anions from His-containing peptides indicates facile rearrangements occurring in peptide radicals and involving the His side chain and the COOH group. The rearrangements occur on a submicrosecond time scale and compete with N−C_α backbone cleavages. The kinetics of the rearrangement depends on the mutual steric accessibility of the imidazole ring and the COOH group. For example, in ALH, where the imidazole ring and COOH group are on the same residue, a H atom migration from the COOH requires a strained eight-membered transition state. This is expected to have a high energy and hamper the rearrangement, as indeed observed. More subtle effects are observed for HAAAL and AAHAL, where the rearrangement depends only mildly on the "linear" distance between the imidazole ring and COOH group. Clearly, the peptide ion and radical secondary structures play a role in determining the mutual accessibility of the histidine ring and the COOH group and hence the kinetics of the H atom migration.

The present results and analysis of His-containing neutral peptide radicals reveal that the rearranged imidazole radicals gain substantial stability. This indicates that His residues may act as radical traps also in ECD and ETD. However, the trapping capability is contingent upon the availability of hydrogen atoms in the peptide C-terminal or side-chain COOH groups to be involved in the catalyzed rearrangement. Effects of the amino acid type, sequence, and peptide secondary structure need to be investigated on a larger scale to explore these novel histidine effects and to determine their role in electron-based methods of peptide fragmentation. In particular, hydrogen bonding between His and acidic amino acid residues (Asp, Glu) may play a role in affecting electron-induced peptide dissociations. Experimental and computational studies to elucidate such interactions are in progress in these laboratories.

Conclusions

Histidine residues in peptide radicals undergo hidden rearrangements upon one-electron reduction of protonated peptides in the gas phase. The rearrangement involves exothermic hydrogen atom migration from a sterically accessible C-terminal carboxyl to the side-chain imidazole ring and is made energetically favorable by dipole−dipole interactions between the COO and imidazoline groups in zwitterionic intermediates. The rearrangement is not observed in the absence of a free COOH group. The carboxyl group mediates exothermic isomerization of the His (3*H*)-imidazoline radical to the more stable (2*H*)-imidazoline isomer. Peptide radical stabilization by hidden H atom migration may explain the previously observed stability of peptide cation radicals upon electron capture and transfer in the gas phase.

Acknowledgment. Research at the University of Washington has received support from the National Science Foundation through Grants CHE-0750048 for experiments and CHE-0342956 for computations. The Department of Chemistry Computer Facility has been jointly supported by the NSF and University of Washington. F.T. thanks the Department of Physics and Astronomy at the University of Aarhus, Denmark, for a visiting professor fellowship from June to August 2007, during which the above-described experiments were carried out. Thanks are also due to A. Ehlerding, Jean A. Wyer, and H. Zettergren for technical assistance. Research at the University of Aarhus was supported by the Danish Natural Research Council (Grants 21-04-0514 and 272-06-0427), Carlsbergfondet (Grant 2006-01-0229), and Lundbeckfonden.

Supporting Information Available: Complete refs 19 and 21, Figures S1−S5, Scheme S1, Tables S1 and S2 with calculated relative energies, and Tables S3−S53 with optimized geometries and total energies. This information is available free of charge via the Internet at www.pubs.acs.org.

JA8036367

(47) Locke, M. J.; McIver, R. T., Jr. *J. Am. Chem. Soc.* **1983**, *105*, 4226.
(48) Note that an exothermic **5** → **12** isomerization is obtained from both B3LYP and MP2/6-311++G(2d,p) calculations (−8 and −11 kJ mol^{-1}, respectively), and thus, it cannot be due to an inadequate treatment of the charge transfer species **12** by DFT calculations.